Journal of Organometallic Chemistry 775 (2015) 55–59

Contents lists available at ScienceDirect

Journal of Organometallic Chemistry

journal homepage: www.elsevier.com/locate/jorganchem

# Effect of diphenylamine substituent on charge-transfer absorption features of the iridium complexes and application in dye-sensitized solar cell

DongDong Wang [a, *], Hua Dong [b], Yong Wu [a, *], Yue Yu [b], GuiJiang Zhou [a], Lu Li [b], ZhaoXin Wu [b, **], Min Gao [a], Geng Wang [a]

[a] Department of Applied Chemistry, School of Science, Xi'an Jiaotong University, Xi'an 710049, China
[b] Key Laboratory for Physical Electronics and Devices of the Ministry of Education, School of Electronic and Information Engineering, Xi'an Jiaotong University, Xi'an 710049, China

ARTICLE INFO

*Article history:*
Received 8 September 2014
Received in revised form
12 October 2014
Accepted 21 October 2014
Available online 30 October 2014

*Keywords:*
Diphenylamine
Iridium complexes
Charge-transfer absorption
Dye-sensitized solar cell

ABSTRACT

The new complex $Ir^{III}$bis(4-diphenylaminophenylpyridinato)-4-carboxylpicolinate (complex **3**) tailored by electron-donating diphenylamine (DPA) was synthesized and characterized for dye-sensitized solar cells (DSSCs) application. The introduction of the DPA moiety to phenylpyridine ligand makes the absorption bands of the complex **3** extend to 650 nm, and adjusts the highest occupied molecule orbital to be mainly localized on DPA-ppy (diphenylaminophenylpyridine) ligands (accounting for 74.44% for one DPA-ppy ligand) while the lowest unoccupied molecule orbital to be lied on the pic (pyridine-2,4-dicarboxyl acid) moiety (96.80%). TD-DFT calculation further shows the charge-transfer transitions from ligand DPA-ppy and Ir atom to the pic anchoring moiety principally contribute to the absorption bands of the complex **3** in the visible region, which is well beneficial to electron injecting into $TiO_2$ film. For DSSCs using complex **3** as sensitizer, the energy conversion efficiency is up to 2.51%, with a short circuit current density of 7.51 mA/cm$^2$ and an open circuit voltage of 0.68 V. These results indicate that it is possible for $Ir^{III}$ complex to achieve more efficient cell parameters if more rational $Ir^{III}$ complexes are developed.



## Introduction

Over past several decades, $Ir^{III}$ complexes have attracted intensive attention for their notable application in organic light-emitting diodes (OLEDs) due to their unique photophysical properties such as owning nearly 100% phosphorescent quantum yields, reasonable excited-state lifetime, excellent color tunability [1–4] and so on. However, such attentions are still steadily reinforced for their extended applications in photocatalyst [5], phosphorescent molecular probes [6,7], photosensitizer for hydrogen production and dye-sensitized solar cells (DSSCs) [8–13] etc. DSSCs are considered as being the most promising solution for harnessing the energy of the sun light and converting it into electricity energy. $Ir^{III}$ complexes have been demonstrated to exhibit several crucial advantages for DSSCs application [8,9] such as having the potential for dual sensitization through LLCT (ligand-to-ligand charge transfer) and MLCT (metal-to-ligand charge transfer) [12], enhanced photostability and the reasonable lifetime of the excited states because of the large d-orbital splitting energy of iridium, which decreases the accessibility of d–d state [13]. However, only few reports illustrated the $Ir^{III}$ complexes for this purpose and cell parameters of them are far from competing with $Ru^{II}$ polypyridyls and other metal complexes such as zinc porphyrin dyes, as well as metal-free organic dyes. Even so, it is an interesting field worth being investigated in depth because the poor performances of the $Ir^{III}$ complex-based DSSCs primarily resulted from their weak absorption in the visible region, leading to poor light-harvesting ability.

Improving absorption of the $Ir^{III}$ complexes in the visible region is a primary concern for them to be applied in DSSCs and other light-harvesting fields. Modifying phenylpyridine (ppy) ligand with oligothiophene pendants [14], oligofluorene segment [15] or using 7-diethylaminocoumarine auxiliary ligand [16] turned out to be effective means for improving absorption response of the $Ir^{III}$ complex to a limited extent. Just recently, we demonstrated that

* Corresponding author. Tel.: +86 02982663914; fax: +86 02982668559.
** Corresponding authors. Tel./fax: +86 02982664867.
*E-mail addresses:* ddwang@mail.xjtu.edu.cn (D. Wang), specwy@mail.xjtu.edu.cn (Y. Wu), zhaoxinwu@mail.xjtu.edu.cn (Z. Wu).

http://dx.doi.org/10.1016/j.jorganchem.2014.10.031
0022-328X/

introducing of dicyanovinyl (DCV) moiety into $Ir^{III}$bis(phenylpyridinato)picolinate ($HIr(ppy)_2pic$), resulting in complex **1** (shown in Scheme 1), could be used as an efficient means to extend absorption response towards longer wavelengths [17]. Furthermore, the derivative of the complex **1** with carboxyl acid anchoring group (complex **2**, shown in Scheme 1) was developed to use for DSSCs [18]. Unfortunately, the cells based on complex **2** present unanticipated poor performance parameters (only 0.19% energy conversion efficiency). We have speculated the poor performances could attribute to the limitation of the electron transfer from $Ir^{III}$ complex to $TiO_2$ film. This is because introduction of dicyanovinyl moiety to ppy induces the two ppy ligands to win significant contribution to the lowest unoccupied orbital (LUMO) of complex **2** aside from the main contribution of the pic (pyridine-2,4-dicarboxyl acid) ligand while electrons located on the DCV-ppy ligands in excited state are difficult to be transferred to $TiO_2$ film due to strong electron-withdrawing ability of the dicyanovinyl moiety. Predictably, introducing a substitute with electron-donating feature into ppy ligands would make the electron distribution of the LUMO orbital be more located on the pic ligand and thus improve cell parameters.

In this paper, we introduced diphenylamine (DPA) moiety with electron-donating property into ppy ligands and developed new $Ir^{III}$ complex **3**, named $Ir^{III}$bis(4-diphenylaminophenylpyridinato)-4-carboxylpicolinate (shown in Scheme 1). Its absorption response characters, electrochemical properties and photovoltaic activities in solar cells were investigated, also compared with the complex **2** reported before.

## Experimental section

### *The synthesis of the $Ir^{III}$ complex **3***

All the reactions were carried under an argon atmosphere and reagents were used without further purification. The $^1H$ NMR and $^{13}C$ spectra were recorded on Bruker Avance 400 MHz spectrometers and HRMS experiments were carried out on a Thermo Scientific LTQ Orbitrap Discovery (Bremen, Germany).

The 0.352 g $IrCl_3 \cdot 3H_2O$ (1.0 mmol) was added to the solution of the *N*,*N*-diphenyl-4-(pyridin-2-yl)aniline (0.805 g, 2.5 mmol) in 32 mL mixed solvent (2-ethoxyethanol:distilled = 3:1) and then the mixtures were refluxed for 24 h under argon. After the reaction was finished, cooling down to room temperature, 150 mL distilled water was added and the precipitate was collected by filtration, washed with water and hexane successively. After drying, the 0.68 g crude product was obtained, which was directly used for next step without further purifying.

The $Ir^{III}$ dimer (0.60 g, 0.35 mmol) was added to the solution of the pyridine-2,4-dicarboxyl acid (0.15 g, 0.88 mmol) in 60 mL 1,2-dichloroethane and the suspension was refluxed for 28 h under argon. Then 1,2-dichloroethane in suspension was evaporated and the resulting precipitate was directly dissolved in mixed solvent of $CH_3OH/CH_2Cl_2$ (1:3) and recrystalled to afford the desired iridium complex. Finally, the product was subjected to flash column chromatography to afford pure product complex **3**: (0.37 g, Yield 53%) $^1H$ NMR (400 MHz, $CDCl_3$-*d*, $\delta$):8.402 (s, 1H),8.201–8.188 (d, 1H, $J = 6.5$), 7.932–7.942 (m, 1H), 7.784–7.928 (m, 2H), 7.716–7.736 (m, 1H), 7.572–7.608 (m, 3H), 7.503 (t,1H), 7.213–7.259 (m, 10H), 7.165–7.179 (d, 1H, $J = 7.0$), 7.002–7.048 (m, 4H), 6.935–6.954 (d, 4H, $J = 9.5$), 6.883–6.902 (d, 4H, $J = 9.5$), 6.778 (t, 1H), 6.377–6.435 (m, 2H), 5.845 (s, 1H), 5.668 (s, 1H); HRMS (ESI): calc. for $C_{53}H_{38}IrN_5O_4$, 1001.2548; found: 1001.2555 ($[M]^+$).

### *Spectroscopy and CV*

The UV absorption in solution and on $TiO_2$-dyes-adsorbed films was measured using Hitachi (U-3310) spectrophotometers and a Varian Cary 500 spectrophotometer, respectively. Emission spectra were recorded with Edinburgh FS920 fluorometers. Cyclic voltammetry (CV) was measured on a Princeton Applied Research Model 273 A electrochemical workstation. A glassy carbon was used as working electrode, and Pt-sheet and Pt-wire as counter-electrode and reference electrode, respectively. The redox measurement for complex **3** was carried out in anhydrous $CH_3CN$ solution with 0.1 M TBAPF6 as supporting electrolyte under scan rate of 100 mV/s. The ferroceninium/ferrocence ($Fc/Fc^+$) was used as internal standard.

### *The preparation and measurement of DSSCs*

DSSCs were fabricated according our published procedures [18]. The electrolyte for all the cells contained 0.6 M 1-butyl-3-methyl imidazolium iodide (BMII), 0.03 M $I_2$, 0.02 M LiI, 0.10 M guanidinium thiocyanate, and 0.5 M 4-tert-butylpyridine in a mixture of acetonitrile and valeronitrile (volume ratio 85:15). The active area of each cell was typically 0.25 $cm^2$. The current–density voltage ($J$–$V$) curves were recorded by a Keithley 2400 source under the illumination of AM 1.5G simulated solar light (Newport-91160). The incident monochromatic photon-to-electron conversion efficiency (IPCE) for the solar cells were measured by a Newport 74125 system (Newport Instruments), in which the intensity of monochromatic light was measured with a Si detector (Newport-71640). The electrochemical impedance spectroscopy (EIS) measurements under illumination were performed on a Zahner IM6e Impedance Analyzer (ZAHNER-Elektrik GmbH & CoKG, Kronach, Germany). The applied voltage bias and the magnitude of the alternative signal were set as −0.70 V and 10 mV, respectively, and the frequency range was 0.1Hz–100 kHz.

### *Computational details of theoretical calculations*

Singlet ground state ($S_0$) geometries of the iridium compounds were fully optimized by using M06 method of density functional theory (DFT). The standard 6-311G(d,p) basis set on non-metal atoms and the relativistic effective core potential (ECP) LANL2DZ on Ir atom were taken in our calculations. The solvent effects were

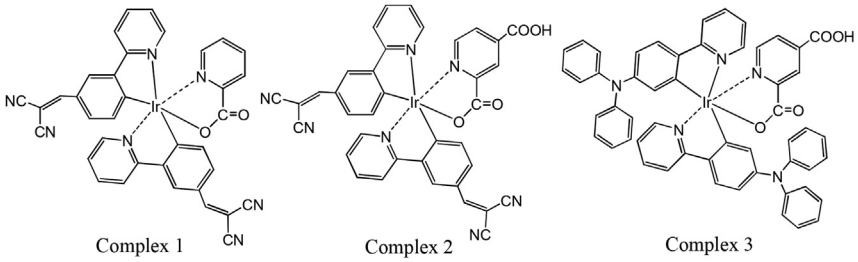


**Scheme 1.** Schematic structure of the $Ir^{III}$ complexes **1**, **2** and **3**.

evaluated with the self-consistent reaction field (SCRF) based on the integral equation formalism of the polarizable continuum model (IEFPCM) in $CH_2Cl_2$ solvent ($\varepsilon = 8.93$). The vertical excitation calculations in $CH_2Cl_2$ for the simulation of absorption spectra were used by the time-dependent (TD) DFT method. All calculations were carried out with the Gaussian 09 program package.

## Results and discussion

### *Photophysical and electrochemical features*

The complex **3** was synthesized according to the previous procedures [19] and the experimental details are presented in the experimental section (See Section 2.1). The Fig. 1 shows the UV–vis absorption spectra of the complex **3** in $CH_3CN$ solution and on $TiO_2$ film, and the corresponding spectra datas are summarized in Table 1, together with that of the complex **2** for comparison. It can be seen that the complex **3** shows slightly weaker absorption bands from 450 nm to 500 nm comparing with that of the complex **2,** but its absorption tail extends to near 650 nm due to a more extended π conjugation of DPA-ppy ligand. Thus, the absorption bands of the complex **3** cover more visible region comparing with nonsubstituted

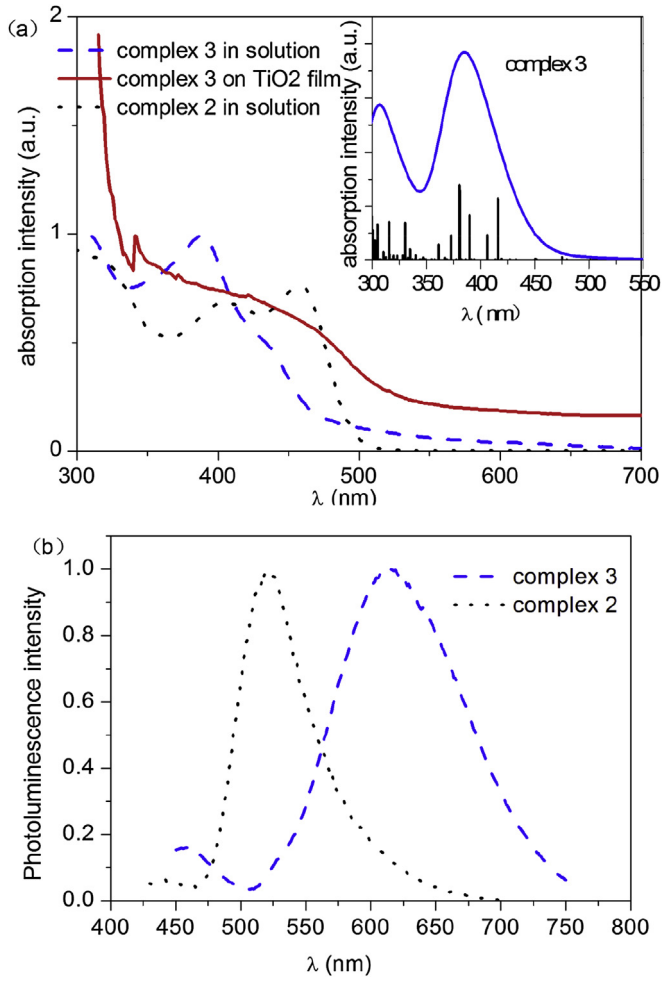


**Fig. 1.** (a) The absorption and (b) photoluminescence spectra of the iridium complexes **3** and **2** in $CH_2Cl_2$ solution, as well as absorption spectra of the complex **3** bounded to $TiO_2$ film. The inset presents simulated absorption spectra donated by blue line and singlet vertical excitation energies represented by black bars. (For interpretation of the references to color in this figure legend, the reader is referred to the web version of this article.)

**Table 1**
The optical, redox and DSSC performance parameters of the $Ir^{III}$ complex **3**, **2** and N719.

| | $\lambda_{abs}$ [nm][a] | $\lambda_{em}$ [nm][b] | $E_{ox}$ [V][c] | $E_{LUMO}$[d] | $J_{sc}$ (mA/cm$^2$)[e] | $V_{oc}$ (V) | FF | $\eta$ (100%) |
|---|---|---|---|---|---|---|---|---|
| Complex **3** | 386, 444 | 614 | 0.65 | 3.07 | 7.51 | 0.68 | 0.49 | 2.51 |
| Complex **2** | 405, 456 | 521/603 | 0.97 | 3.27 | 0.46 | 0.58 | 60.3 | 0.19 |
| N719 | | | | | 13.15 | 0.70 | 0.65 | 6.01 |

[a] Absorption and emission spectra were measured in $CH_2Cl_2$ solution.
[b] Emission spectra were measured in $CH_2Cl_2$ solution.
[c] $E_{ox}$ is oxidation potential measured in $CH_3CN$ solution and the potential value is relative to $Fc^+/Fc$.
[d] The LUMO was estimated by formula: $E_{LUMO}$ (eV) = $E_{Ox} - E_{0\text{-}0}$, $E_{0\text{-}0}$ is determined according to the intersection of the absorption and emission spectra in $CH_2Cl_2$ solution.
[e] Performances of DSSCs were measured under AM 1.5G conditions (100 mW/cm$^2$) with an active area of 0.25 cm$^2$, Iodine electrolyte: 0.6 M 1-butyl-3-methyl imidazolium iodide (BMII), 0.03 M $I_2$, 0.02 M LiI, 0.10 M guanidinium thiocyanate, and 0.5 M 4-tert-butylpyridine in a mixture of acetonitrile and valeronitrile (volume ratio 85:15).

$HIr(ppy)_2pic$ with absorption cutoff wavelength of 500 nm [20]. When it was assembled on $TiO_2$ film, a red-shifted absorption bands up to 500 nm was observed. Upon photoexcitation, the complex **3** presents red phosphorescent emission with a peak value 614 nm (shown in Fig. 1b), about 109 nm bathochromic-shift in comparison with that of $HIr(ppy)_2pic$ and $E_{0\text{-}0}$ transition energy thus was estimated to be 2.38 eV. The red-shift emission of $Ir^{III}$ complexes was always observed when electron-donating group is introduced to phenyl moiety of the ppy ligand. Density functional theory (DFT) calculations show the π-orbitals of DPA-ppy ligand contribute 74.44% to the HOMO (the highest occupied orbital) of complex **3** and Ir d-orbital presents only 8.38% contribution. The LUMO is almost completely contributed by π orbitals of the pic moiety, accounting for 96.80% (shown in Fig. 2 and Table S1 of the supplemental information) while the LUMO of nonsubstituted $HIr(ppy)_2pic$ is more delocalized over the two ppy moieties and pic ligand. This difference can be attributed to the fact that introduction of DPA to phenyl moiety of ppy could enhance electron rich property of DPA-ppy ligand due to electron-donating nature of DPA and thus induce the redistribution of electron density distributed on ligand units of $Ir^{III}$ complex. This means that introducing of DPA moiety into ppy unit makes electronic structure of the $Ir^{III}$ complex **3** be more favorable for electron injecting into $TiO_2$ film when applied to DSSCs. However, the HOMO orbital of the complex **2** is comparably contributed by Ir atom and π orbitals located on DCV-ppy ligands and its LUMO orbital is delocalized over the two DCV-ppy ligands and the pic ligand (Fig. 2), implying unfavorable electronic structure for DSSCs applications.

We further calculated the nature of the lowest excited state based on the time-dependent density functional theory (TD-DFT) to assist interpretation of these experimental spectra. The calculation absorption features of the complex **3** in $CH_2Cl_2$ solution and transitions with significant oscillator strength are presented in inset of the Fig. 1a and Table S2, respectively, (Supplemental information). The calculated maximum absorption peaks and absorption region (300–450 nm) with significant intensity well coincide with the experimental results. The absorption peaks at low energy region above 400 nm have mainly LLCT and MLCT character. For example, the calculated absorption peak at 517.9 nm ($f = 0.0016$, 60% contribution from HOMO → LUMO transition) and 475.1 nm ($f = 0.0098$, 85% contribution from HOMO-1 → LUMO transition) are mainly contributed by LLCT between the DPA-ppy ligand and the pic moieties, which has positive effect on reducing disfavorable charge recombination usually occurring in $Ru^{II}$-based cells due to MLCT character [21,22]. As is indicated by the computed results that the HOMO and HOMO-1 molecular orbital have 74.44% and 75.39% contribution localized on the DPA-ppy unit, respectively, while

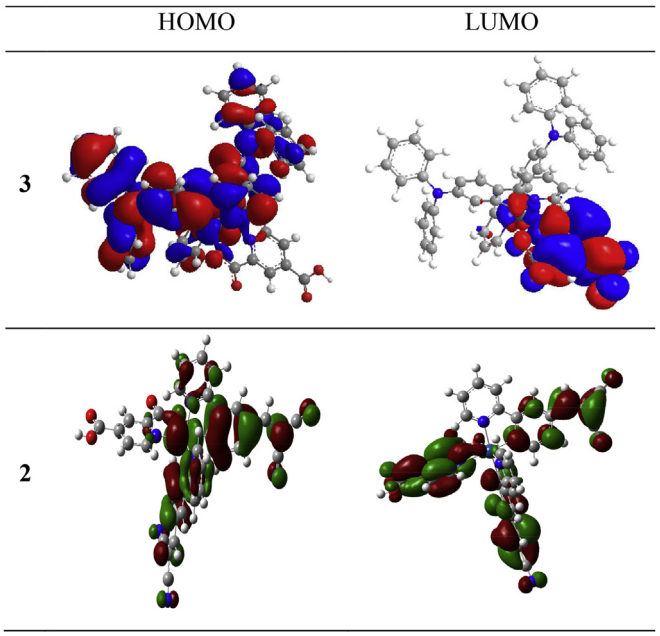


**Fig. 2.** The calculated contours of the HOMO and LUMO orbitals of the iridium complexes **3** and **2**.

LUMO molecule orbital has 96.80% contribution localized on the pic moiety, as shown in Fig. 2. The slight higher energy absorption peak 450.5 nm ($f$ = 0.0034, HOMO-2 → LUMO (69%)), 419.3 nm ($f$ = 0.0035, HOMO-3 → LUMO (92%)) and 381.2 nm ($f$ = 0.2569, HOMO-4 → LUMO (53%)) are mainly contributed by MLCT occurring from Ir atom to the pic moiety because HOMO-2, HOMO-3 and HOMO-4 molecular orbitals contain 37.81%, 69.46% and 73.85% contributions from central Ir atom, respectively. Both transition paths from MLCT and LLCT are benefiting for electron injection in DSSC application. At UV region near or below 400 nm, the intra-ligands $\pi \rightarrow \pi^*$ transitions primarily contribute to significant absorption response such as the computed absorption peaks 405.8 nm ($f$ = 0.0925, HOMO → LUMO + 2(59%)) and 389.6 nm ($f$ = 0.1671, HOMO-1 → LUMO + 1(50%)). It should be noted that inter-ligands charge–transfer transition among the DPA-ppy units presents most of the highest oscillator intensity such as 415.9 nm ($f$ = 0.229, HOMO → LUMO + 1(60%)), 380.1 nm ($f$ = 0.278, HOMO-1 → LUMO + 2(40%)), indicating this transition also is an important source for absorption response in UV region.

Cyclic voltammogram (CV) of the complex **3** in MeCN solution was further performed to get the experimental HOMO energy levels based on the ionization potential for the first oxidation, and CV curve corrected according to the potentials of the $Fc^+/Fc$ (0.16 V) is shown in Fig. 3. The irreversible redox processes centered at 0.65 V vs $Fc^+/Fc$ were observed with positive scan for complex **3**, because oxidation involves the electron-rich DPA substitute on the ppy (Fig. 2) [23]. Similarly, an irreversible single reduction process occurs at −2.25 V vs $Fc^+/Fc$ at negative scan, which could be assigned to a pic-based process. Based on the measured oxidation potentials in solution, the HOMO energy levels of the complex **3** was determined as 5.45, 0.17 eV difference from the computed result.

*Photovoltaic activities*

The absorption response of the complex **3** above 400 nm has much more LLCT features, that is mainly charge transfer bands from the DPA-ppy unit to pic anchoring unit, which makes electron-injecting into $TiO_2$ be highly favorable when excited. It is therefore expect that more improved cell parameters should be achieved

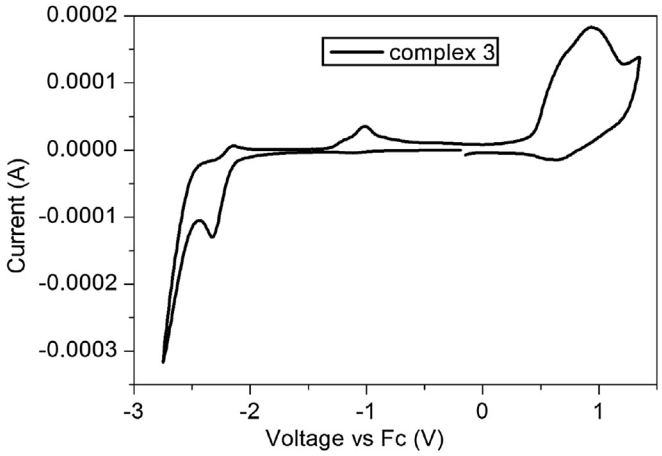


**Fig. 3.** The cyclic voltammograms of the iridium complexes **3** in $CH_3CN$ solution.

comparing with that of the complex **2**. The characteristics of the photovoltaic cells measured under AM 1.5G conditions (100 mW/cm$^2$) are given in Table 1 and Fig. 4. The complex **3** presented a short circuit current density of 7.51 mA/cm$^2$ and an open circuit voltage of 0.68 V, about 140 mV higher than that of the early reported results that used iridium complexes as photosensitizer [8,9,12], and also significantly excelled that of the complex **2**, only 0.46 mA/cm$^2$ and 0.58 mV. The IPCE curves of the complex **3**-based cell exhibited comparable intensity with that of N719-based cell and extended to 650 nm, indicating that the weak tailing absorption features also considerably contribute to the visible light collection. Just as expected, the cell of the complex **3** presents overall energy conversion efficiency of 2.51%, thirteen times as much as that of the complex **2**.

The electrochemical impedance spectroscopy (EIS) of the DSSCs under illumination condition was further performed to get insight into the electron transport processes in cells. The radium of the Nyquist plot (shown in Fig. 5) in the middle semicircle usually reflects the electron recombination impedance [24,25] and a larger radius means a higher resistance of electron recombination at the $TiO_2$/dye/electrolyte interface. In Fig. 5, this radius of the complex **3** is clearly larger than that of the N719, implying that it has higher electron recombination impedance. This could be explained that the excited states of the complex **3** owns considerable LLCT features while that of the N719 principally has MLCT character, in which the electrons in $TiO_2$ film injected from dyes are inclined to recombination with a redox couple presented in electrolyte. But, the $V_{oc}$ (0.68 V) of the complex **3**-based cell is slightly lower than that of the N719-based cell (0.70 V), which is inconsistent with the order of the electron-recombined resistance at the $TiO_2$/dye/electrolyte interface. We speculate that the $Ir^{III}$ complex **3** shows lower light harvesting capacity comparing with N719 and thus under the same the illumination condition, the $TiO_2$ film collect relative lesser electrons for complex **3**-based cell than that for N719 device, therefore leading to slightly lower open-circuit voltage. The complex **2**-based cell show the highest electron recombined resistance but the lowest $V_{oc}$ among three devices. The reason may be same as that.

## Conclusion

In summary, we introduced DPA moiety into prototype complex $Ir^{III}$bis(phenylpyridinato)-4-carboxylpicolinate to tune the absorption response character by resorting its electron donating nature and make resulted complex $Ir^{III}$bis(4-diphenylaminophenylpyridinato)-4-carboxylpicolinate (complex **3**) win favorable charge-transfer

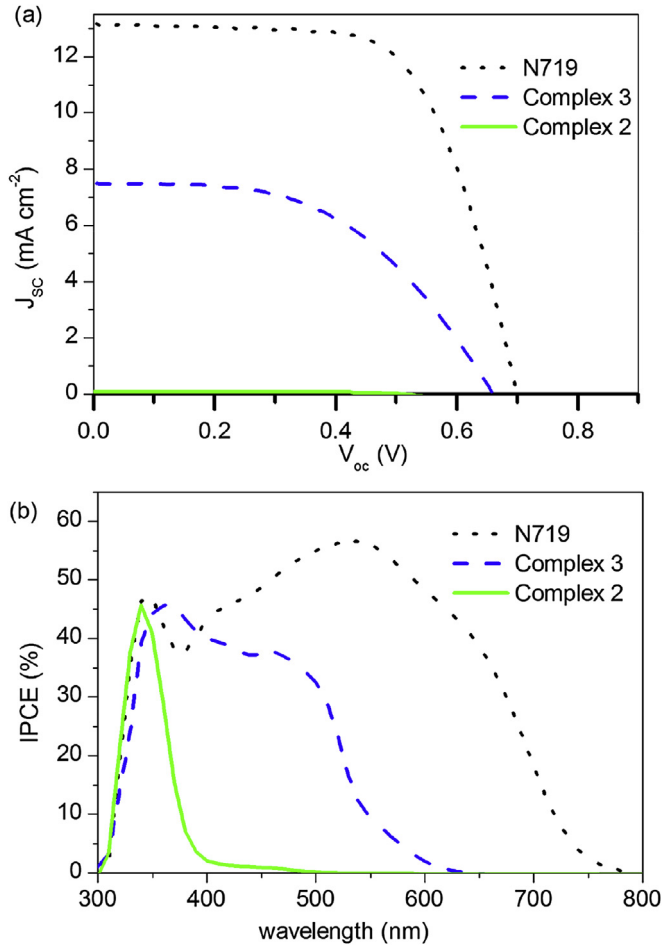


**Fig. 4.** (a) IPCE spectra and (b) photocurrent density–voltage characteristics curves for DSSC devices recorded under illumination of simulated solar light (AG 1.5G, 100 mW/cm$^2$).

bands for electron-injecting into $TiO_2$ film when applied to DSSCs. The resulting complex **3** shows extending absorption response to 650 nm and presents red phosphorescent emission with a peak value 614 nm. Density functional theory (DFT) calculations show the charge-transfer transition from the ligand DPA-ppy and Ir atom to the pic anchoring unit principally contribute to the absorption response

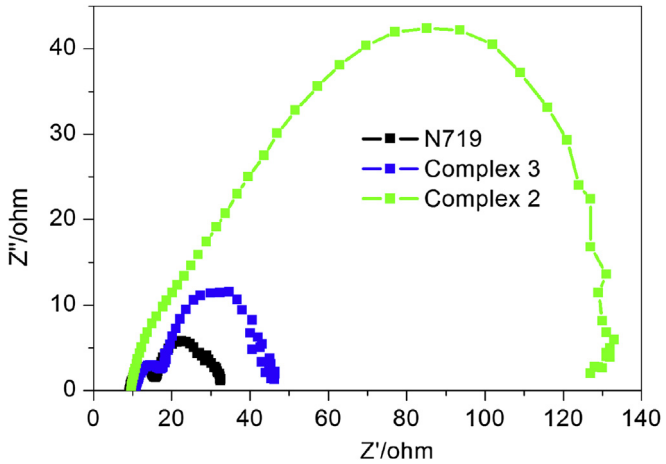


**Fig. 5.** Electrochemical impedance spectra measured under AM 1.5G conditions (100 mW cm$^{-2}$).

in the visible light region (above 400 nm), which is favorable for electron injecting into $TiO_2$ film. The DSSCs using $Ir^{III}$ complex **3** as photosensitizer exhibited a widely responding IPCE characteristic (up to 650 nm) and presented a $V_{oc}$ of 0.68 V, $J_{sc}$ of 7.51 mA/cm$^2$ and 2.51% conversion efficiency. These results indicate that it is possible for $Ir^{III}$ complex to achieve more efficient cell parameters if more rational $Ir^{III}$ complexes are developed. Thus, the dual sensitization property and the well electrochemical stability of the $Ir^{III}$ complexes would be greatly beneficial to the improvement of the cell parameters in comparison with Ru complexes.

## Acknowledgments

This work has been supported by the Fundamental Research Funds for the Central Universities (Grant. Nos. 08143034), the Basic Research Program of China (2013CB328705), National Natural Science Foundation of China (Grant Nos. 61275034 and 61106123).

## Appendix A. Supplementary data

Supplementary data related to this article can be found at http://dx.doi.org/10.1016/j.jorganchem.2014.10.031.

## References

[1] M.A. Baldo, S. Lamansky, P.E. Burrows, M.E. Thompson, S.R. Forrest, Appl. Phys. Lett. 75 (1999) 4–6.
[2] S. Lamansky, P. Djurovich, D. Murphy, F. Abdel-Razzaq, H.E. Lee, C. Adachi, P.E. Burrows, S.R. Forrest, M.E. Thompson, J. Am. Chem. Soc. 123 (2001) 4304–4312.
[3] A. Tsuboyama, H. Iwawaki, M. Furugori, T. Mukaide, J. Kamatani, S. Igawa, T. Moriyama, S. Miura, T. Takiguchi, S. Okada, M. Hoshino, K. Ueno, J. Am. Chem. Soc. 125 (2003) 12971–12979.
[4] E. Holder, B.M.W. Langeveld, U.S. Schubert, Adv. Mater. 17 (2005) 1109–1121.
[5] S. Park, D. Bezier, M. Brookhart, J. Am. Chem. Soc. 134 (2012) 11404–11407.
[6] K.K.W. Lo, W.K. Hui, C.K. Chung, K.H.K. Tsang, T.K.M. Lee, C.K. Li, J.S.Y. Lau, D.C.M. Ng, Coord. Chem. Rev. 250 (2006) 1724–1736.
[7] K.K.W. Lo, C.K. Chung, T.K.M. Lee, L.H. Lui, K.H.K. Tsang, N.Y. Zhu, Inorg. Chem. 42 (2003) 6886–6897.
[8] Y.J. Yuan, J.Y. Zhang, Z.T. Yu, J.Y. Feng, W.J. Luo, J.H. Ye, Z.G. Zou, Inorg. Chem. 51 (2012) 4123–4133.
[9] Z.J. Ning, Q. Zhang, W.J. Wu, H. Tian, J. Organomet. Chem. 694 (2009) 2705–2711.
[10] C. Dragonetti, A. Valore, A. Colombo, S. Righetto, V. Trifiletti, Inorg. Chim. Acta 388 (2012) 163–167.
[11] Y. Shinpuku, F. Inui, M. Nakai, Y. Nakabayashi, J. Photochem. Photobiol. A Chem. 222 (2011) 203–209.
[12] E.I. Mayo, K. Kilsa, T. Tirrell, P.I. Djurovich, A. Tamayo, M.E. Thompson, N.S. Lewis, H.B. Gray, Photochem. Photobiol. Sci. 5 (2006) 871–873.
[13] E. Baranoff, J.H. Yum, M. Graetzel, M.K. Nazeeruddin, J. Organomet. Chem. 694 (2009) 2661–2670.
[14] K.R. Schwartz, R. Chitta, J.N. Bohnsack, D.J. Ceckanowicz, P. Miro, C.J. Cramer, K.R. Mann, Inorg. Chem. 51 (2012) 5082–5094.
[15] Q. Yan, Y. Fan, D. Zhao, Macromolecules 45 (2012) 133–141.
[16] A.J. Hallett, B.D. Ward, B.M. Kariuki, S.J.A. Pope, J. Organomet. Chem. 695 (2010) 2401–2409.
[17] D.D. Wang, Y. Wu, B. Jiao, H. Dong, G.J. Zhou, G. Wang, Z.X. Wu, Org. Electron. 14 (2013) 2233–2242.
[18] D.D. Wang, H. Dong, X.Y. Zhang, Wu, S.H. Shen, B. Jiao, Z.X. Wu, M. Gao, G. Wang, Sci. China Chem. (2014) in press.
[19] D.D. Wang, Y. Wu, H. Dong, Z.X. Qin, D. Zhao, Y. Yu, G.J. Zhou, B. Jiao, Z.X. Wu, M. Gao, G. Wang, Org. Electron. 14 (2013) 3297–3305.
[20] E. Baranoff, B.F.E. Curchod, F. Monti, F. Steimer, G. Accorsi, I. Tavernelli, U. Rothlisberger, R. Scopelliti, M. Gratzel, M.K. Nazeeruddin, Inorg. Chem. 51 (2012) 799–811.
[21] A. Hagfeldt, G. Boschloo, L. Sun, L. Kloo, H. Pettersson, Chem. Rev. 110 (2010) 6595–6663.
[22] P.G. Bomben, T.J. Gordon, E. Schott, C.P. Berlinguette, Angew. Chem. Int. Ed. 50 (2011) 10682–10685.
[23] M. Gennari, F. Legalite, L. Zhang, Y. Pellegrin, E. Blart, J. Fortage, A.M. Brown, A. Deronzier, M.N. Collomb, M. Boujtita, D. Jacquemin, L. Hammarstrom, F. Odobel, J. Phys. Chem. Lett. 5 (2014) 2254–2258.
[24] M. Adachi, M. Sakamoto, J.T. Jiu, Y. Ogata, S. Isoda, J. Phys. Chem. B 110 (2006) 13872–13880.
[25] C. He, L. Zhao, Z. Zheng, F. Lu, J. Phys. Chem. C 112 (2008) 18730–18733.